Parametric Driving of Dark Solitons in Atomic Bose-Einstein Condensates

N. P. Proukakis, N. G. Parker, C. F. Barenghi, and and C. S. Adams

Department of Physics, University of Durham, South Road, Durham, DH1 3LE, United Kingdom
School of Mathematics and Statistics, University of Newcastle, Newcastle upon Tyne, NE1 7RU, United Kingdom
(Received 22 March 2004; published 23 September 2004)

A dark soliton oscillating in an elongated harmonically confined atomic Bose-Einstein condensate continuously exchanges energy with the sound field. Periodic optical paddles are employed to controllably enhance the sound density and transfer energy to the soliton, analogous to parametric driving. In the absence of damping, the amplitude of the soliton oscillations can be dramatically reduced, whereas with damping, a driven soliton equilibrates as a *stable* soliton with lower energy, thereby extending the soliton lifetime up to the lifetime of the condensate.

DOI: 10.1103/PhysRevLett.93.130408 PACS numbers: 03.75.Lm, 05.45.Yv, 42.81.Dp, 47.35.+i

Dark solitons [1] are an important manifestation of the intrinsic nonlinearity of a system and arise in diverse systems such as optical fibers [2], waveguides [3], surfaces of shallow liquids [4], magnetic films [5], and atomic Bose-Einstein Condensates (BECs) [6]. Dark solitons are dynamically unstable in higher than one-dimensional (1D) manifolds (e.g., snake instability in 3D leading to decay into vortex rings [7–9]). Solitons in 1D geometries experience other instabilities [10], whose nature depends on the system: For example, dark solitons in optical media are prone to nonlinearity-induced changes in the refractive index [1], whereas in harmonically trapped atomic BECs they experience dynamical instabilities due to the *longitudinal* confinement [9,11–15], as well as thermodynamic [16] and quantum [17] effects. Instabilities lead to dissipation via the emission of radiation. Compensation against dissipative losses by parametric driving has been demonstrated in some of the above media [4,18]. The aim of this Letter is to discuss this effect in the context of atomic BECs.

In atomic gases, the snake instability [8] can be suppressed in elongated, quasi-1D geometries [19], with thermal instabilities minimized at temperatures $T \ll T_c$ (where T_c is the BEC transition temperature). In this limit, a dark soliton oscillating in a harmonically-confined BEC continuously emits radiation (in the form of sound waves) due to the inhomogeneous background density [11]. The sound remains confined and reinteracts with the soliton, leading to periodic oscillations of the soliton energy [14]. In this Letter, we propose the controlled amplification of the sound field at a particular frequency, and illustrate the resulting transfer of energy into the soliton, in close analogy to established parametric driving techniques [4]. Energy is pumped into the sound field via periodically modulated "paddles", located towards the condensate edge (Fig. 1). If the drive frequency is nearly resonant with the soliton oscillation frequency, one observes significant energy transfer to the soliton. In the absence of dissipation, this leads to a dramatic reduction in the amplitude of the soliton oscillations. Under dissipative conditions, the damped soliton equilibrates as a *stable* soliton with lower energy, with its lifetime extended up to the condensate lifetime. Moreover, suitable engineering of the phase of the driving field (relative to the soliton oscillations) can maintain the soliton energy at its initial value for times significantly longer than the undriven soliton lifetime.

Our analysis is based on the cylindrically-symmetric 3D Gross-Pitaevskii Equation (GPE) describing the evolution of the macroscopic order parameter $\psi(\rho, z)$ of an elongated 3D atomic BEC

$$i\hbar\frac{\partial\psi}{\partial t} = -\frac{\hbar^2}{2m}\nabla^2\psi + V\psi + g|\psi|^2\psi - \mu\psi, \qquad (1)$$

where m is the atomic mass, $V = V_T(\mathbf{r}) + V_D(\mathbf{r})$, $V_T(\mathbf{r}) = (m/2)(\omega_z^2 z^2 + \omega_\perp^2 \rho^2)$ is the harmonic confining potential of longitudinal (transverse) frequency ω_z ($\omega_\perp$), where $\omega_z \ll \omega_\perp$, and $V_D(\mathbf{r})$ is the drive potential (Eq. (3)). The nonlinearity arises from effectively repulsive atomic interactions yielding a scattering amplitude $g = 4\pi\hbar^2 a/m$,

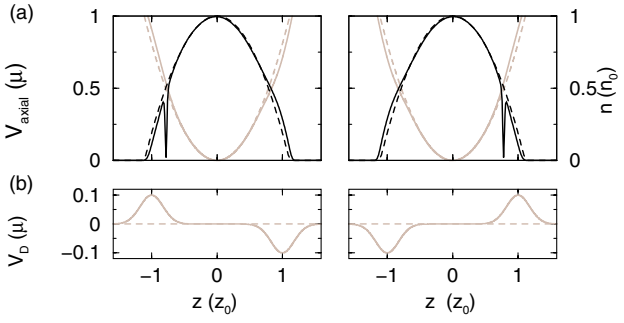

FIG. 1 (color online). Schematic of parametric driving: (a) Total axial potential (gray lines, left axis) and density (black lines, right axis) of perturbed harmonic trap with propagating dark soliton (solid lines), at 2 times (left/right plots) corresponding to maximum drive amplitudes. (b) Corresponding drive potentials (solid gray, $\alpha > 0$). Dashed lines denote density/potential in the unperturbed harmonic trap.

where $a > 0$ is the s-wave scattering length. The chemical potential is given by $\mu = gn_0$, where n_0 is the peak atomic density.

Dark soliton solutions are supported by the 1D form of Eq. (1) in the absence of external confinement ($V = 0$). On a uniform background density n, a dark soliton with speed v and position $(z - vt)$ has the form,

$$\psi(z,t) = \sqrt{n}e^{-i(\mu/\hbar)t}\left\{\beta \tanh\left[\beta\frac{(z-vt)}{\xi}\right] + i\left(\frac{v}{c}\right)\right\} \quad (2)$$

where $\beta = \sqrt{1-(v/c)^2}$, and the healing length $\xi = \hbar/\sqrt{\mu m}$ characterizes the soliton width. The soliton speed $v/c = \sqrt{1-(n_d/n)} = \cos(S/2)$ depends on the total phase slip S across the center and the soliton depth n_d (with respect to the background density), with the limiting value set by the Bogoliubov speed of sound $c = \sqrt{\mu/m}$. The energy of the unperturbed dark soliton, Eq. (2), is given by $E_s^0 = (4/3)\hbar cn[1-(v/c)^2]^{3/2}$. The drive potential

$$V_D = \alpha \sin(\omega_D t)\left[e^{-(z+z_0)^2/w_0^2} - e^{-(z-z_0)^2/w_0^2}\right] \quad (3)$$

consists of two periodically-modulated Gaussian paddles, with amplitude α, at positions $\pm z_0$, oscillating in antiphase at a *fixed* frequency ω_D, close to the soliton frequency (Fig. 1). Such a set up could be created by time-dependent red and blue detuned laser beams with beam waist w_0.

In our Letter, the dark soliton is defined as the density deviation from the unperturbed density (in the absence of the soliton) within the "soliton region" R: $[z_s - 5\xi, z_s + 5\xi]$, where z_s the instantaneous position of the local density minimum. This "perturbed" soliton includes sound excitations located within the soliton region. The motion and stability of a quasi-1D dark soliton is well parametrized by its energy. In order to compare the quasi-1D soliton energy to the analytical homogeneous 1D energy, the soliton dynamics are parametrized in terms of the "on-axis" ($\rho = 0$) soliton energy $E_s = \int_R \{\varepsilon[\psi(0,z)] - \varepsilon[\psi_{bg}(0,z)]\}dz$, where $\varepsilon(\psi) = \hbar^2/(2m)|\nabla\psi|^2 + V|\psi|^2 + (g/2)|\psi|^4$ and $\varepsilon[\psi_{bg}(0,z)]$ is the corresponding background fluid contribution [14,15,20].

Dissipationless Regime:— Consider first the case of no dissipation. In the absence of V_D, the soliton oscillates at $\omega_{sol} = \omega_z/\sqrt{2}$ [9,11–16], emitting sound waves which oscillate at the trap frequency ω_z. This frequency mismatch means that the soliton propagates through a periodically-modulated background density, leading to a *weak* periodic modulation of the soliton energy [Fig. 2(a), curves (i)). The amplitude of this modulation is enhanced by the coupling between longitudinal and transverse degrees of freedom [12,14].

To demonstrate substantial energy transfer into the soliton, we start with a low energy shallow soliton (speed $v_0 = 0.75c$ at $z = 0$). Applying the drive potential induces an *additional*, more pronounced, periodic background density modulation and a time dependence in the soliton oscillation frequency, which is found to vary less than 10% from its unperturbed value ω_{sol}. As a result, the relative phase between the drive and the soliton oscillations, which determines the direction of energy flow between soliton and sound, becomes time dependent. Beginning with the drive out-of-phase with the soliton oscillations, the soliton initially acquires energy, up to time t_0, after which it begins to lose energy, and the cycle repeats [curves (ii) in Fig. 2(a)]. There is good agreement between the 3D "on-axis" energy (black lines) and the corresponding energy of the pure 1D simulations (gray lines) (3D results feature an additional small amplitude oscillation due to longitudinal-transverse coupling). The corresponding beating in the soliton oscillation amplitude is shown in Fig. 2(b) (gray line). This beating effect can be visualized as the periodic cycling between the initial low energy dark soliton, and the nearly stationary high energy soliton, somewhat analogous to the cycling of a driven condensate between the "no-vortex" and "single-vortex" configurations [21]. A soliton of higher energy can be created by removing the drive potential after a certain pumping time [Fig. 2(a), curves (iii)]. A nearly stationary soliton (black line in Fig. 2(b)), can be created

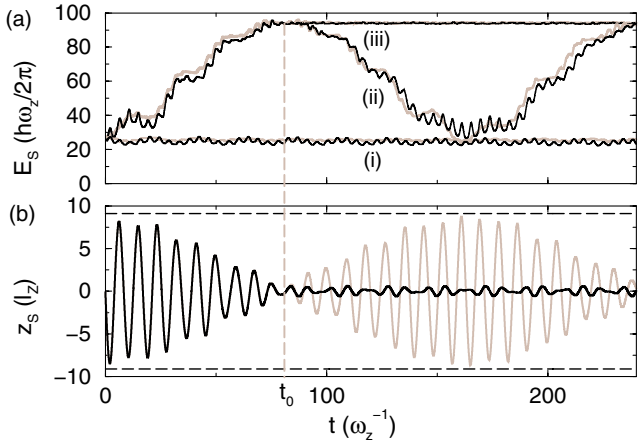

FIG. 2 (color online). (a) 'On-axis" quasi-1D soliton energy for (i) undriven case, (ii) continuous driving and (iii) driving switched off at $t_0 = 80\omega_z^{-1}$, based on simulations of the 3D cylindrically-symmetric GPE (black lines) and 1D GPE (gray lines) for a soliton with initial speed $v_0 = 0.75c$. (b) Longitudinal soliton oscillations with continuous driving (gray line), and driving switched off at t_0 (vertical gray line) under the 3D GPE. Dashed lines indicate the initial amplitude. The trap strength is determined from the chemical potential: Quasi-1D: $\mu_{3D} = 8\hbar\bar{\omega}$ with $\bar{\omega} = (\omega_z\omega_\perp^2)^{1/3}$ and $\omega_\perp/\omega_z = 250$. Pure 1D: $\mu_{1D} = 70\hbar\omega_z$ for which the 1D density matches the quasi-1D longitudinal density. Drive parameters: $\omega_D = 0.98\omega_{sol}$, $\alpha = 0.1\mu_{1D}$, $w_0 = 3.2l_z$, $z_0 = 10.7l_z$ with $l_z = \sqrt{\hbar/(m\omega_z)}$ the longitudinal harmonic oscillator length.

by stopping the drive when the soliton has acquired its maximum energy.

The soliton dynamics depend sensitively on the parameters of the driving field. Firstly, the pumping should take place outside of the range of the soliton oscillations (i.e., $z_0 > 9l_z$ for $v_0 = 0.75c$). Otherwise, the soliton traverses the Gaussian bumps, leading to "dephasing" of emitted sound waves and subsequent soliton decay [15]. The transfer of energy between the soliton and the sound field depends on the phase of the drive relative to the soliton oscillations, and hence on the drive potential seen by the soliton at the extrema of its oscillatory motion. This parameter depends on the drive frequency ω_D, the amplitude of the potential modulation α, the range of the potential w_0, its location z_0, and the initial soliton speed v_0. For given a choice of α, w_0, z_0, and v_0, there is a resonance in the sound energy absorbed as a function of the drive frequency ω_D as illustrated by the open circles in Fig. 3. The maximum pumping does not arise precisely at ω_{sol}, due to the additional frequency modification induced by the perturbing potential. Importantly, the width of the resonance for which the transferred soliton energy reaches half its maximum value (FWHM), is reasonably broad ($\sim 10\%\omega_{sol}$). Alternative schemes for pumping energy into the soliton (e.g. via one off- center paddle, or with $\alpha < 0$), lead to a delayed and less efficient energy transfer, while periodically displacing the trap causes no net increase in the soliton energy.

Dissipative Regime:— In a realistic quasi-1D system, both condensate and soliton are prone to damping, e.g., due to a small thermal cloud [16]. To estimate the effect of dissipation, we introduce a phenomenological damping term $\hbar\gamma\partial\psi/\partial t$ on the left-hand side of Eq. (1) [22]. In the absence of driving, this term leads to an approximately exponential decay of the soliton energy, modified by the oscillatory motion of the soliton (dashed line in Fig. 4(a)). Dissipation also damps the sound field, leading to a narrowing and a shift (towards ω_{sol}) of the resonance in the drive frequency (gray data in Fig. 3).

Stabilization Against Decay:— For a high energy soliton, continuous parametric driving counterbalances damping initially (solid line in Fig. 4(a) up to $\omega_z t \sim 90$), but subsequently the soliton starts to decay ($90 < \omega_z t < 170$), thereby changing both the amplitude and the phase of the soliton oscillations [11,14]. The evolution in the relative phase between the drive and the soliton oscillations eventually enables the soliton to gain energy again. After a few gain-loss cycles, the initially deep ($v_0 = 0.3c$) soliton of energy $E_s \approx 80\hbar\omega_z$ *equilibrates* as a shallower soliton of energy $E_s \approx 35\hbar\omega_z$ (corresponding to $v_0 \approx 0.7c$).

Stabilization at Fixed Energy:— Some applications may require a soliton maintained at fixed energy. For this, one must balance the competing effects of driving and dissipation. This can be achieved by rephasing the drive relative to the soliton oscillations at appropriate times, as demonstrated by the solid line in Fig. 4(b) for a sequence of four rephasing operations. In principle, such stabilization can be extended to the duration of the condensate lifetime. In an experiment, one actually measures the position of the soliton (rather than its energy) [6]. Hence, rephasing could be performed by monitoring the amplitude of the soliton oscillations and adjusting the

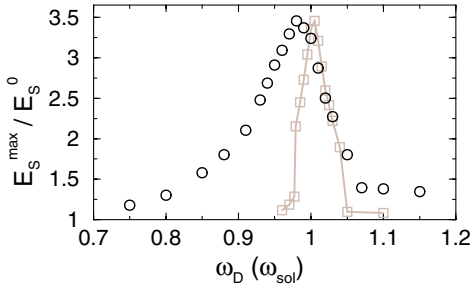

FIG. 3 (color online). Optimized ratio of maximum pumped energy E_s^{max} to initial soliton energy E_s^0 for a $v_0 = 0.75c$ soliton as a function of drive frequency for (i) no damping (black circles), or (ii) with damping $\gamma = 5 \times 10^{-4}$ (gray squares). This value of γ leads to the same soliton lifetime as for the undriven $0.3c$ soliton in Fig. 4. Results based on pure 1D GPE for the case of Fig. 2.

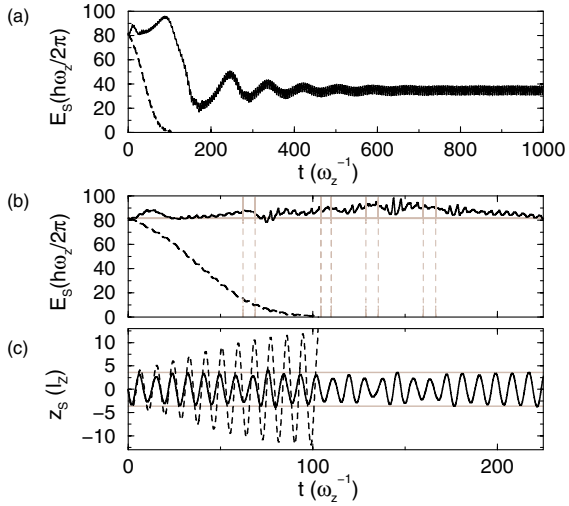

FIG. 4 (color online). (a) Soliton energy ($v_0 = 0.3c$) for a dissipative system ($\gamma = 10^{-3}$) in the presence (solid line) or absence (dashed) of continuous driving ($\omega_D = \omega_{sol}$, $z_0 = 7.1l_z$). The driven soliton stabilizes at $E_s \approx 35\hbar\omega_z$. (b) Energy of a $v_0 = 0.3c$ soliton with parametric driving (solid black), undergoing rephasing during the periods between adjacent dashed gray lines. Dashed black line as in (a). (c) Driven (solid line) and undriven (dashed line) soliton trajectories for case (b). In (b), (c), horizontal gray lines indicate the initial soliton energy and oscillation *amplitude*. Results based on the 1D GPE, with other parameters as in Fig. 2.

drive phase, so that the soliton oscillation amplitude remains constant. Figure 4(c) shows the oscillation amplitude of the parametrically driven soliton (solid black line), which is very similar to the undamped undriven case, and is clearly distinct from the undriven dissipative motion (dashed black line), whose amplitude increases until the soliton decays at $\omega_z t = 105$.

Finally, we discuss the relevance of the proposed scheme to current experiments with atomic BECs. Given a longitudinal confinement $\omega_z = 2\pi \times 10$ Hz, the presented results correspond to $\omega_\perp = 2\pi \times 2500$ Hz, a linear "on-axis" density $n = 5 \times 10^7 (1.5 \times 10^7) \mathrm{m}^{-1}$ of ^{23}Na (^{87}Rb), and harmonic oscillator time $\omega_z^{-1} \approx 15$ ms. In Fig. 4 ($\gamma = 10^{-3}$), this corresponds to a soliton lifetime of $\sim$1s, consistent with the theoretical predictions for solitons in quasi-1D geometries [9,11,16]. The paddle beams have a waist $w_0 = 20\mu$m and maximum amplitude $\alpha = 7\hbar\omega_z$ located around $z_0 = 7l_z$. The results presented here also hold for smaller aspect ratios (e.g., $\omega_\perp/\omega_z = 50$). Since, for a given aspect ratio, higher frequencies correspond to faster timescales, the technique presented here is not sensitive to the particular soliton lifetime. Increasing γ beyond an upper limit (i.e., large dissipation), renders it practically impossible to increase or stabilize the soliton energy.

We have shown that, in the case of a dark soliton oscillating in a harmonically trapped Bose-Einstein condensate, the addition of two out-of-phase Gaussian potentials, with amplitude modulated periodically at a fixed frequency close to the soliton frequency, pumps energy into the soliton. This parametric driving technique can stabilize the soliton against decay for timescales comparable to the condensate lifetime. Optimization of the phase of the drive can further force the soliton to maintain its initial energy for *at least* a few times its natural lifetime. Both effects should be observable in current experiments.

We acknowledge discussions with D. J. Frantzeskakis and P. G Kevrekidis and the UK EPSRC for funding.

[1] Y. S. Kivshar and B. Luther-Davies, Phys. Rep. **298**, 81 (1998).
[2] D. Krökel *et al.*, Phys. Rev. Lett. **60**, 29 (1998).
[3] G. A. Swartzlander Jr. *et al.*, Phys. Rev. Lett. **66**, 1583 (1991).
[4] B. Denardo *et al.*, Phys. Rev. Lett. **64**, 1518 (1990).
[5] M. Chen *et al.*, Phys. Rev. Lett. **70**, 1707 (1993).
[6] S. Burger *et al.*, Phys. Rev. Lett. **83**, 5198 (1999);J. Denschlag *et al.*, Science **287**, 97 (2000);Z. Dutton, M. Budde, C. Slowe, and L. V. Hau, Science **293**, 663 (2001).
[7] A. V. Mamaev, M. Saffman, and A. A. Zozulya, Phys. Rev. Lett. **76**, 2262 (1996).
[8] D. L. Feder *et al.*, Phys. Rev. A **62**, 053606 (2000);B. P. Anderson *et al.*, Phys. Rev. Lett. **86**, 2926 (2001);J. Brand and W. Reinhardt, Phys. Rev. A **65**, 043612 (2002).
[9] A. E. Muryshev, H. B. van Linden van den Heuvell, and G. V. Shlyapnikov, Phys. Rev. A **60**, R2665 (1999).
[10] P. G. Kevrekidis and D. J. Frantzeskakis, Mod. Phys. Lett. B **18**, 173 (2004).
[11] T. Busch and J. R. Anglin, Phys. Rev. Lett. **84**, 2298 (1999).
[12] G. Huang, J. Szeftel, and S. Zhu, Phys. Rev. A **65**, 053605 (2002).
[13] D. J. Frantzeskakis *et al.*, Phys. Rev. A **66**, 053608 (2002);V. A. Brazhnyi and V. V. Konotop, Phys. Rev. A **68**, 043613 (2003).
[14] N. G. Parker, N. P. Proukakis, M. Leadbeater, and C. S. Adams, Phys. Rev. Lett. **90**, 220401 (2003).
[15] N. G. Parker, N. P. Proukakis, M. Leadbeater, and C. S. Adams, J. Phys. B **36**, 2891 (2003);N. G. Parker *et al.* J. Phys. B **37**, S175 (2004);N. P. Proukakis *et al.*, J. Opt. B **6**, S380 (2004).
[16] P. O. Fedichev, A. E. Muryshev and G. V. Shlyapnikov, Phys. Rev. A **60**, 3220 (1999);A. E. Muryshev *et al.*, Phys. Rev. Lett. **89**, 110401 (2002).
[17] J. Dziarmaga *et al.*, J. Phys. B **36**, 1217 (2003).
[18] C. Elphick and E. Meron, Phys. Rev. A **40**, 3226 (1989);F. K. Abdullaev and S. K. Tadjimuratov, Opt. Commun. **116**, 179 (1995);A. D. Kim, W. L. Kath and C. G. Goedde, Opt. Lett. **21**, 465 (1996);P. Coullet *et al.*, Phys. Rev. Lett. **65**, 1352 (1990);D. V. Skryabin *et al.*, Phys. Rev. E **64**, 056618 (2001);I. V. Barashenkov *et al.*, Phys. Rev. Lett. **90**, 054103 (2003).E. Falcon *et al.*, Phys. Rev. Lett. **89**, 204501 (2002); W. Chen *et al.*,Phys. Lett. A **208**, 197 (1995).
[19] A. Gorlitz *et al.*, Phys. Rev. Lett. **87**, 130402 (2001);F. Schreck *et al.* Phys. Rev. Lett. **87**, 080403 (2001);H. Ott *et al.* Phys. Rev. Lett. **87**, 230401 (2001).
[20] L. D. Carr, J. Brand, S. Burger, and A. Sanpera, Phys. Rev. A **63**, 051601 (2001).
[21] B. M. Caradoc-Davies, R. J. Ballagh and K. Burnett, Phys. Rev. Lett. **83**, 895 (1999).
[22] S. Choi, S. A. Morgan and K. Burnett, Phys. Rev. A **57**, 4057 (1998);M. Tsubota, K. Kasamatsu and M. Ueda, Phys. Rev. A **65**, 023603 (2002).